Computer simulation for the precipitation process of $Ni_{75}Al_{7.5}V_{17.5}$ alloy*

LI Yongsheng**, CHEN Zheng, LU Yanli, WANG Yongxin and ZHANG Jianjun

(Department of Material Science and Engineering, Northwestern Polytechnical University, Xi'an 710072, China)

Received May 18, 2004; revised July 15, 2004

Abstract The precipitation mechanism of $Ni_{75}Al_{7.5}V_{17.5}$ alloy above the $L1_2$ instability line, between the $L1_2$ and $D0_{22}$ instability lines and below the $D0_{22}$ instability line are studied using microscopic phase-field kinetic equation. This paper is aimed at investigating the effect of temperature on precipitation mechanism and morphological evolution of the alloy. Our simulations demonstrate that the precipitation is a mixed mechanism of non-classical nucleation growth and spinodal decomposition above the $L1_2$ instability line. It needs certain thermal fluctuations for nucleation and the number of θ phases is small at this temperature. The precipitation mechanism of γ' phase is congruent ordering followed by spinodal decomposition, and θ phase is a mixed mechanism of non-classical nucleation growth and spinodal decomposition between the $L1_2$ and $D0_{22}$ instability lines. The mechanism below the $D0_{22}$ instability line is similar to that between the $L1_2$ and $D0_{22}$ instability lines. With the decrease of the temperature, ordering and phase separation becomes fast, the dimension of γ' phase becomes small, the shape transforms from equiaxed to block, the dimension of θ phase becomes large and the shape transforms from strip to circle.

Keywords: precipitation mechanism, atomic configuration, order parameter, $Ni_{75}Al_{7.5}V_{17.5}$ alloys, computer simulation.

The precipitation morphology has important effect on the capability of alloy. Since computer simulation of the early precipitation mechanism of alloy can offer theoretical guidance for real experiment, computer simulation technique of the microscopic structure is developing quickly in recent years, such as the widely used Molecular Dynamics and Monte Carlo method[1,2]. The microscopic phase-field kinetic model has made great success in simulating the precipitation morphological evolvement[3~5]. In this paper, we use the ternary system microscopic diffusion kinetic equation which was developed by Chen[6,7]. The equation was transformed into the Fourier space, so the 3D problem can be solved in the reciprocal space, and intuitionistic atomic configuration through 2D projection can be obtained. The precipitation mechanism and ordering for two phases can be studied by the atomic configuration and order parameter.

This paper first studied the effect of temperature on precipitation mechanism and morphological evolvement of ternary $Ni_{75}Al_{7.5}V_{17.5}$ alloy. We selected several representative points within the two phase field labeled by small stars in the phase diagram shown in Fig. 1[8], the temperature for points a, b and c is 1250 K, 1180 K and 1000 K respectively. There are two phases in $Ni_{75}Al_{7.5}V_{17.5}$ alloy at every temperature, which are the γ' (Ni_3Al) and θ (Ni_3V) phases. The γ' phase has the L12 structure and the θ phase has the $D0_{22}$ structure[9].

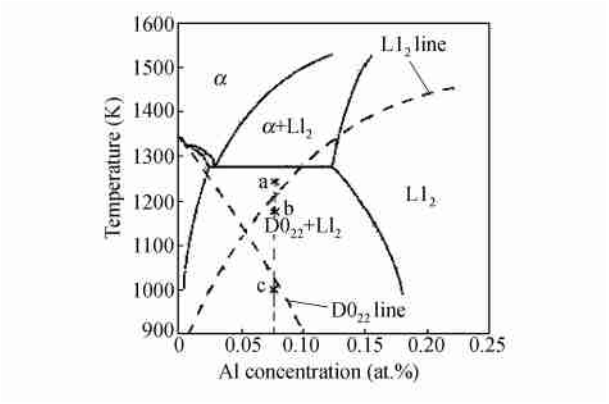

Fig. 1. Pseudobinary Ni_3Al-Ni_3V phase diagram.

1 Microscopic phase-field kinetic model

Microscopic phase-field kinetic equation is based on the Onsage and Ginzburg-Landau equation[10,11], the atomic structure and alloy morphology are described by a single-site occupation probability function $x(r, t)$, which is the probability that a given lattice site r is occupied by an atom at time t. The change

* Supported by the National Natural Science Foundation of China (Grant No. 50071046), and the National High Technology Research Development Program of China (Grant No. 2002AA331051)

** To whom correspondence should be addressed. E-mail: llyss2008@sina.com

rate of these probabilities is linearly proportional to the thermodynamics driving force

$$\frac{\partial x(r,t)}{\partial t} = \sum_{r'} L(r-r') \frac{\delta F}{\delta x(r',t)}, \quad (1)$$

where F is the function of the free energy of $x(r',t)$, $L(r-r')$ is the symmetry matrix of the microscopic kinetic related to the probability of an elementary diffusion jump from site r to r' per unit of time.

Microscopic diffusion equation was first put forward by Khachaturyan[10]. The ternary system microscopic was developed by Chen[6,7]. The kinetic equation is

$$\begin{cases} \dfrac{dP_A(r,t)}{dt} = \dfrac{1}{k_B T}\sum_{r'}\left[L_{AA}(r-r')\dfrac{\partial F}{\partial P_A(r',t)} + L_{AB}(r-r')\dfrac{\partial F}{\partial P_B(r',t)}\right], \\ \dfrac{dP_B(r,t)}{dt} = \dfrac{1}{k_B T}\sum_{r'}\left[L_{BA}(r-r')\dfrac{\partial F}{\partial P_A(r',t)} + L_{BB}(r-r')\dfrac{\partial F}{\partial P_B(r',t)}\right], \end{cases} \quad (2)$$

where $P_A(r,t)$, $P_B(r,t)$ represent the probability of finding the A, B atoms at a given lattice site r at a given time t. Since for ternary system there are three kinds of atoms, we use $P_C(r,t)$ as the occupation probabilities of the C atom. Then $P_A(r,t)+P_B(r,t)+P_C(r,t)=1$. Only two equations are independent of each other at each lattice site.

F is the total free energy of the system based on the mean-field approximation,

$$\begin{aligned} F = & -\frac{1}{2}\sum_{r}\sum_{r'}[V_{AB}(r-r')P_A(r)P_B(r') \\ & + V_{BC}(r-r')P_B(r)P_C(r') \\ & + V_{AC}(r-r')P_A(r)P_C(r')] \\ & + k_B T\sum_{r}[P_A(r)\ln(P_A(r)) \\ & + P_B(r)\ln(P_B(r)) + P_C(r)\ln(P_C(r))], \end{aligned} \quad (3)$$

where $V_{\alpha\beta}$ is the interaction energies between α and β (A, B or C).

Through Fourier transform, the equation transforms from a 3D and a non-linear partial differential equation into a 2D and linear constant differential equation, so the computation work can be greatly decreased. At the same time, we can obtain the intuitionistic atomic configuration. In addition, any prior assumption on the new phase structure or transformation path is unnecessary. The possible nonequilibrium phases, atomic clustering and ordering can be described automatically.

2 Simulation results and discussion

In our simulation, the color scheme used to depict the picture is as follows: The color assigned to each lattice site is a mixture of red, green and blue, equal to the occupation probability at that site of aluminum, vanadium and nickel, respectively. Thus, if the occupation probability of aluminum is 1.0, then that site is assigned the color red, and so on. Therefore, the θ phase appears to be green, the γ' phase appears to be red and all the nickel sites in both phases appear to be blue, and a blue background is formed.

2.1 The precipitation mechanism above the $L1_2$ instability line

The simulation uses 128× 128 lattice points, and the timestep is 0.0002. It is difficult for nucleation at this region, so we initially add certain timesteps of thermal fluctuations[12]. Plate IA is the morphology evolvement at different timesteps at 1250 K. There are compositional fluctuations with small range and large amplitude that appear in Plate IA(a), the thermal fluctuations are 3000 timesteps. Our simulation indicates that if the thermal fluctuation is less than this value, the system will turn back to the disorder state. The initial θ phase decays and the solute spareness region is formed as the simulation continues, which are labeled with arrows in Plate IA(a)~(c). However, the γ' phase continues to grow and the ordered phase is formed finally. This is because the driving force for γ' phase is larger than that of θ phase in this region. The ordered phase is circular (see Plate IA(c)), and there exists a transition region of several lattices wide between the ordered phases, so the precipitation is a non-classical nucleation[13]. Finally, there are a few θ phases as shown in Plate IA(d), and the dimension of γ' phase is very large and the order-disorder region exists between the γ' phase.

Figure 2 is the variations of composition and long range order parameter. The composition order parameter has some fluctuations initially and falls then, which is consistent with the atomic configuration. The center of the order parameter begins to rise but does not reach the maximum, which indicates that the nucleus begins to form and the ordered phase is

nonstoichiometric. With time progressing, the order parameter continues to rise and extend at the same time, which has the double characteristic of spinodal decomposition and non-classical nucleation. Finally, the order parameter reaches the maximum and forms the stoichiometric ordered phase. Form the atomic configuration and the order parameter, we can conclude that the precipitation mechanism is the mixed style of non-classical nucleation and spinodal decomposition.

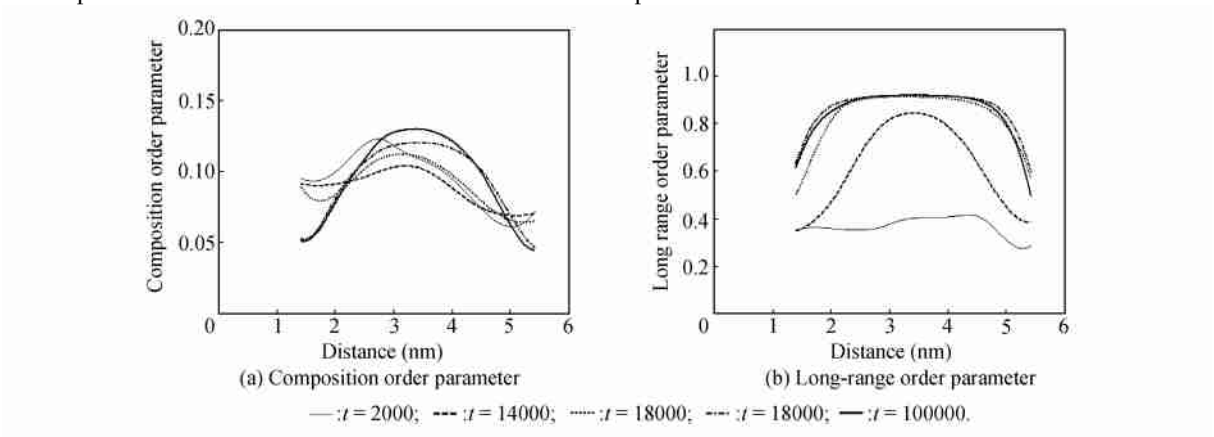

Fig. 2. Order parameter profiles across the ordered phase above the $L1_2$ instability line at different times.

2.2 The precipitation mechanism between $L1_2$ and DO_{22} instability lines

Different from the precipitation process of 1250 K, there are no composition fluctuations at the beginning, for the thermal fluctuation is very little. The γ' phase is just formed and the occupation probability of Al atom is low, it is the nonstoichiometric ordered phase (see Plate IB(a)). As time proceeds, the γ' phase grows and forms anti-phase domain boundaries (APBs), the θ phase separates to the APBs and starts to nucleate and grow (see Plate IB (c), (d)).

Because the driving force is larger than that of the above $L1_2$ instability line, the precipitation rate is fast and the quantity of θ phase increases. Figure 3 (a), (b) show the variations of composition and long range order parameter of γ' phase at different times. At the beginning, the composition order parameter has no change while the LRO parameter reaches the maximum. It can be confirmed that the ordering is essentially congruent and the nonstoichiometric ordered phase is formed at this stage. After this course, the composition order parameter rises gradually and the width does not change, which demonstrates that the spinodal decomposition happens. The LRO extends and the ordered phase grows. Finally, the stoichiometric ordered phase is formed. Therefore, the precipitation order is a congruent ordering followed by spinodal decomposition.

The changes of the order parameters inside the θ phase are similar to but more obvious than that of γ' phase at 1250 K (see Fig. 3(c), (d)). Both the order parameters rise and extend at the same time and finally reach the maximum. It can be seen that the precipitation is a mixed type of non-classical nucleation and spinodal decomposition. It can also be found that the LRO in θ phase has a minimum and it shifts to left, which shows that the θ phase nucleates at the boundary of γ' phase and the growing direction is perpendicular to the γ' phase.

2.3 The precipitation mechanism below the DO_{22} instability line

From the atomic evolvement configuration (see Plate IC) and order parameter (see Fig. 4), we can see that the precipitation mechanism of two phases is similar to that of 1180 K to some degree, but the trend of nucleation and growth of θ phase is more obvious, for the composition order parameter is much narrower. There are some differences for the precipitation, the γ' phase precipitates fastly and the quantity increases, and the dimension becomes smaller compared with that of 1180 K. As shown in Plate IC(d), the quantity of θ phase increases and the dimension becomes large and the shape trends to circle. This is because the driving force increases with the decrease of the temperature. At the initial stage, the center is lower than the boundary of the composition order parameter of θ phase (see Fig. 4(a)). The reason for this is that the V atom diffuse to the boundary and the Al atom cannot complement in

time. For θ phase, the precipitation mechanism is congruent ordering followed by spinodal decomposition. For γ' phase, the precipitation mechanism is non-classical nucleation and spinodal decomposition.

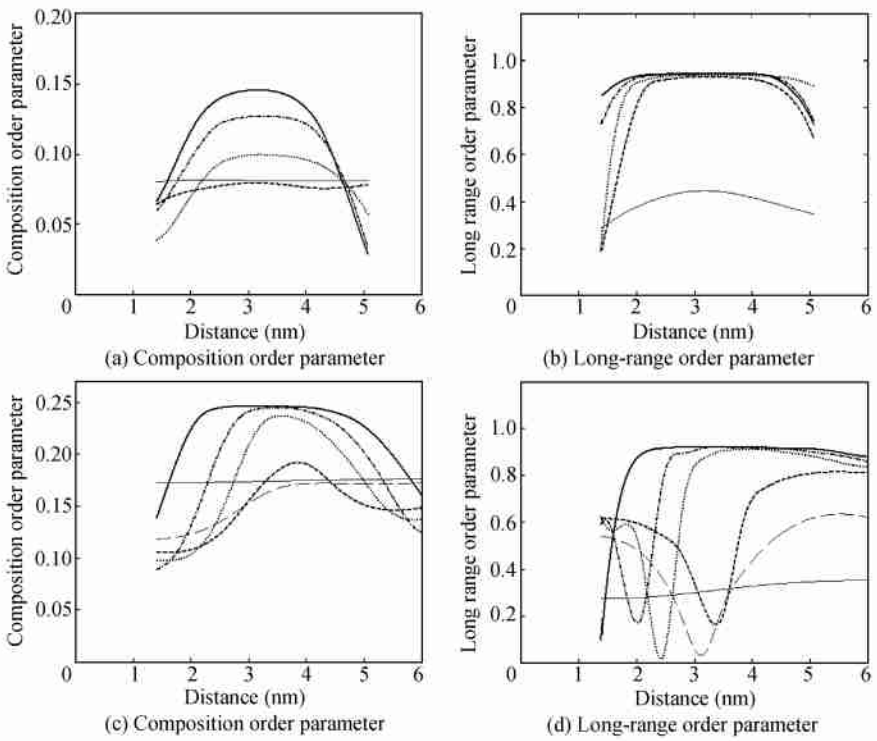

In (a), (b), — :t = 20000; --- :t = 23000; ····· :t = 40000; -·-· :t = 60000; — :t = 100000.
In (c), (d), — :t = 16000; — :t = 20000; --- :t = 23000; ····· :t = 40000; -·-· :t = 60000 — :t = 100000.

Fig. 3. Order parameter profiles across the θ ordered phase between the $L1_2$ and DO_{22} instability lines at different times.

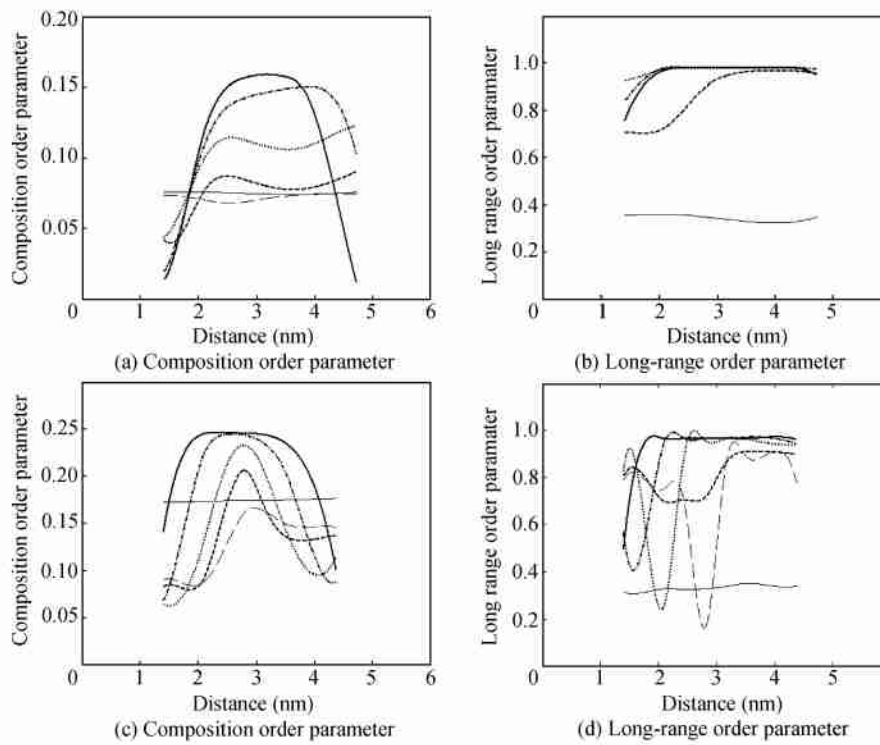

In (a), — :t = 2000; --- :t = 5000; --- :t = 10000; ····· :t = 20000; -·-· :t = 35000; — :t = 100000.
In (b) , — :t = 2000; --- :t = 12500; ····· :t = 25000; -·-· :t = 37500; — :t = 100000.
In (c),(d), — :t = 2500; --- :t = 7500; --- :t = 12500; ····· :t = 25000; -·-· :t = 37500; — :t = 100000.

Fig. 4. Order parameter profiles across the γ' and θ ordered phases below the DO_{22} instability line at different times.

Bendersky and his co-worker studied the precipitation process of Ni-Al-V alloys with TEM and X-ray diffraction, which demonstrated the precipitation order and transformation path of two phases[14]. Zapolsky studied the co-existent system of Ni_3Al and Ni_3V with the 3DAP technique[15]. The precipitation process predicted by our simulation agrees with the experimental observations, and the precipitation mechanism is clarified further.

3 Conclusions

(i) Nucleation needs certain timesteps of thermal fluctuations and there are only a few θ phases above $L1_2$ instability. The shape of γ' phase is circular. The precipitation mechanism is a mixed style of non-classical nucleation growth and spinodal decomposition.

(ii) The precipitation needs very little thermal fluctuation between the $L1_2$ and $D0_{22}$ instability lines. The θ phase nucleates at the APBs of γ' phase and is in strips. The γ' phase is shaped like blocks and the precipitation mechanism is congruent ordering followed by spinodal decomposition. The precipitation mechanism of θ phase is a mixed style of non-classical nucleation growth and spinodal decomposition.

(iii) Both phases precipitate fast and the quantities increase below the $D0_{22}$ instability line. The dimension of γ' phase diminishes but the θ phase increases and the shape develops to a circle. The precipitation mechanisms of γ' and θ phase are similar to that of between the $L1_2$ and $D0_{22}$ instability lines but the nucleation growth is more obvious for θ phase.

References

1 Pareige, C. Ordering and phase separation in Ni-Cr-Al: Monte-Carlo simulation Vs 3D atom probe. Acta Mater. 1998, 47(6): 1889.

2 Sankey, F. et al. An initio multicenter tight-binding model for molecular-dynamic simulations and other applications in covalent systems. Phys. Rev. B, 1989(40): 3979.

3 Chen, L. Q. et al. Computer simulation of structural transformations during precipitation of an ordered intermetallic phase. Acta Metall. Mater., 1991, 39(11): 2533.

4 Li, X. L. et al. Computer simulation for early precipitation of δ' (Al_3Li). Progress in Natural Science, 2002, 12(1): 74.

5 Zhao, Y. H. et al. Computer simulation of strain-induced morphological transformation of coherent precipitates. J. Univ. Sci. Technol. Beijing, 2003, 10(4): 55.

6 Chen, L. Q. A computer simulation technique for spinodal decomposition and ordering in ternary systems. Scripta Metallurgica et Materialia, 1993, 29(5): 683.

7 Chen, L. Q. Computer simulation of spinodal decomposition in ternary systems. Acta Metall. Mater., 1994, 42(10): 3503.

8 Poduri, R. et al. Computer simulation of atomic ordering and compositional clustering in the pseudobinary Ni_3Al-Ni_3V system. Acta Mater., 1998, 46(5): 1719.

9 Zhao, Y. H. et al. Atomic-scale computer simulation for early precipitation process of $Ni_{75}Al_{10}V_{15}$ alloy. Progress in Natural Science, 2004, 14(3): 241.

10 Khachaturyan, A. G. Theory of Structural Transformation in Solids. New York: Wiley, 1983, 129.

11 Wen, Y. H. et al. Microstructure evolution during the $\alpha_2 \rightarrow \alpha_2 + O$ transformation in TI-AL-NB alloys: phase-field simulation and experimental validation. Acta Mater., 2000, 48: 4125.

12 Li, X. L. et al. Transition from metastability to instability in dynamics for the precipitation of δ' (Al_3Li). Rare Metals, 2001, 20(4): 240.

13 Haasen, P. et al. Phase Transformation in Materials (in Chinese), Beijing: Science Press, 1998, 219.

14 Bendersky, L. K. et al. Solid-Solid Phase Transformation. Warrendale, PA: TMS, 1994, 899.

15 Zapolsky, H. et al. Atom probe analyses and numerical calculation of ternary phase diagram in Ni-Al-V system. Calphad, 2001, 25(1): 125.

Plate I

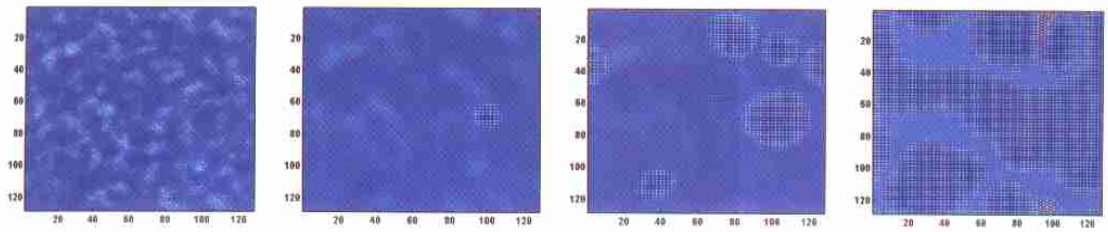

(a) (b) (c) (d)

A. Temporal evolution of the occupation probabilities above the $L1_2$ instability line for $Ni_{75}Al_{7.5}V_{17.5}$.

(a) t =3000; (b) t =9000; (c) t =16000; (d) t =100000.

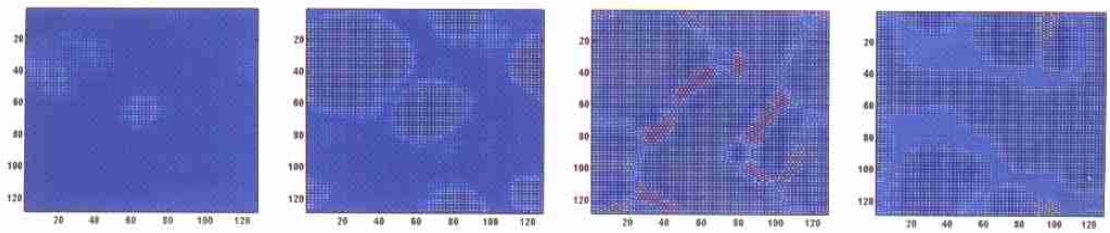

(a) (b) (c) (d)

B. Temporal evolution of the occupation probabilities between the $L1_2$ and $D0_{22}$ instability lines for $Ni_{75}Al_{7.5}V_{17.5}$.

(a) t =17000; (b) t =20000; (c) t =50000; (d) t =100000.

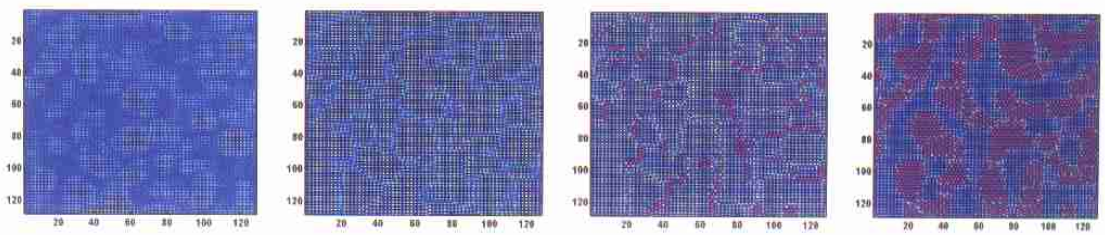

(a) (b) (c) (d)

C. Temporal evolution of the occupation probabilities below $D0_{22}$ instability line for $Ni_{75}Al_{7.5}V_{17.5}$.

(a) t =4000; (b) t =6000; (c) t =10000; (d) t =100000.